Separation Science and Technology
Publication details, including instructions for authors and subscription information:
http://www.informaworld.com/smpp/title~content=t713708471

Effects of Centrifuge Shape on the Separation of a Mixture

H. Edward Donley[a]; William H. Ingham[b]
[a] Department of Mathematics and Computer Science, Harrisonburg, Virginia [b] Department of Physics, James Madison University, Harrisonburg, Virginia

To cite this Article Donley, H. Edward and Ingham, William H.(1987) 'Effects of Centrifuge Shape on the Separation of a Mixture', Separation Science and Technology, 22: 7, 1691 — 1710
To link to this Article: DOI: 10.1080/01496398708058429
URL: http://dx.doi.org/10.1080/01496398708058429

SEPARATION SCIENCE AND TECHNOLOGY, **22(7)**, pp. 1691-1710, 1987

Effects of Centrifuge Shape on the Separation of a Mixture

H. EDWARD DONLEY

DEPARTMENT OF MATHEMATICS AND COMPUTER SCIENCE

WILLIAM H. INGHAM

DEPARTMENT OF PHYSICS

JAMES MADISON UNIVERSITY
HARRISONBURG, VIRGINIA 22807

Abstract

This paper examines the effect of centrifuge shape on the separation time for a two-phase mixture in a centrifuge with a meridional barrier. The work is based on the results of Greenspan and Ungarish. Both the inner radius of the centrifuge and the shape of the lids affect the separation time. It was found, through numerical experiments, that altering the shapes of the lids yields more enhancement than increasing the inner radius. Also, centrifuges with parallel, linear, sloped lids give better results than those with lids having slight or moderate curves superimposed on the linear lids. The curvature appears to interfere with the Boycott effect. However, a sawtooth pattern superimposed on the linear lids is an improvement over the linear lids.

1. INTRODUCTION

In this paper we consider a centrifuge that is filled with an incompressible fluid containing small suspended particles of a second phase, either solid particles or droplets of a second, immiscible, incompressible fluid. We examine the effect of centrifuge shape on the time required for separation to occur. Our work is based on that of Greenspan and Ungarish (*1*) who have already simplified the governing equations and have analyzed several important centrifuge shapes.

The Boycott effect in gravitational settling, most recently studied by

Acrivos and Herbolzheimer (*2*), suggests that alteration of centrifuge geometry can enhance separation. Suppose particles are initially dispersed throughout a less dense, incompressible fluid in a gravitational field. The Boycott effect occurs when this mixture is in a container with inclined walls as in Fig. 1. As the particles separate from the inwardly inclined walls, a boundary layer of pure fluid forms. This layer is less dense than the adjoining mixture. The resultant pressure gradient causes the pure fluid in the boundary layer to flow upward along the wall, forming a pure fluid layer at the top. This forces the mixture downward, accelerating the downward flux of the particles.

As is shown in Refs. *1* and *3*, an axisymmetric centrifuge cannot produce an analogous enhancement in settling, but a centrifuge with a meridional barrier can do so. The barrier allows an azimuthal pressure gradient to counteract the Coriolis force, permitting flows reminiscent of the Boycott effect. In this paper we consider only centrifuges with meridional barriers.

2. GOVERNING EQUATIONS

This section follows the derivation and notation of Greenspan and Ungarish (*1*). Asterisks denote dimensional variables. Suppose the dispersed particles each have constant radius a^* and density ρ_D^*, and they occupy volume fraction α^*. The subscript D distinguishes the dispersed phase from the continuous phase, designated by the subscript C. Variables characterizing the mixture have no subscripts; e.g.,

$$\rho^* = (1 - \alpha)\rho_C^* + \alpha\rho_D^*$$

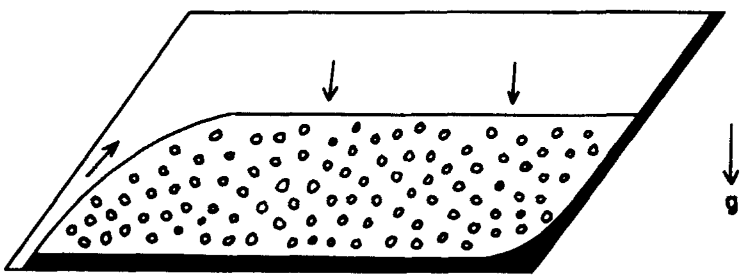

FIG. 1. Boycott effect in gravitational settling.

In a cylindrical coordinate system (r^*,θ^*,z^*) rotating with angular velocity Ω^*, we let $\mathbf{q}^*$ denote the fluid velocity and

$$\mathbf{j}^* = j_r^*\hat{\mathbf{r}} + j_\theta^*\hat{\boldsymbol{\theta}} + j_z^*\hat{\mathbf{z}}$$

denote the volume flux. In the flows we consider, the relative velocity,

$$\mathbf{q}_R^* = \mathbf{q}_D^* - \mathbf{q}_C^*$$

is determined by the drag-bouyancy balance. Furthermore, we suppose that the effective viscosity of the fluid depends only on the local volume fraction. In that case we can approximate $\mathbf{q}_R^*$ by

$$\mathbf{q}_R^* = \varepsilon\beta\Omega^* r^* f(\alpha)\hat{r}$$

where

$$\varepsilon = \frac{\rho_D^* - \rho_C^*}{\rho_C^*}, \qquad \beta = \frac{2a^{*2}}{9\nu^*/\Omega^*}$$

and ν^* is the kinematic viscosity of the fluid. It is assumed that the particle Taylor number, β, which measures the ratio of the Coriolis force to Stokes drag, is small. The factor $f(\alpha)$ in the expression for $\mathbf{q}_R^*$ allows for modification of the drag on a sphere when other spheres are nearby. For consistency with the usual expression for Stokes drag, the infinite-dilution limit of f must be unity:

$$\lim_{\alpha\to 0} f(\alpha) = 1$$

For definiteness in what follows, we adopt the expression suggested by Ishii and Chawla (*4*),

$$f(\alpha) = (1-\alpha)\left(1 - \frac{\alpha}{\alpha_M}\right)^{2.5\alpha_M}$$

Here α_M is the maximal-packing volume fraction for the particles.

To obtain dimensionless variables, we scale velocity by $|\varepsilon|\beta\Omega^* r_0^*$, a typical value of $|\mathbf{q}_R^*|$; length by r_0^*, the outer radius of the centrifuge; time by $1/(|\varepsilon|\beta\Omega^*)$; and density by ρ_C^* (*1*). The dimensionless continuity equations are

$$\frac{\partial\alpha}{\partial t} + \operatorname{div} j_D = 0 \tag{2.1}$$

$$\text{div}\, j = 0 \tag{2.2}$$

Taking the stress term to be that of a constant-viscosity Newtonian fluid, the momentum equation for the mixture is

$$(1 + \varepsilon\alpha)2\hat{z}\times\mathbf{q} + |\varepsilon|\beta\left[\frac{\partial\mathbf{q}}{\partial t} + \tfrac{1}{2}\nabla(\mathbf{q}\cdot\mathbf{q}) + (\nabla\times\mathbf{q})\times\mathbf{q}\right]$$

$$= -\frac{1}{\beta}\nabla P + \frac{s}{\beta}\alpha r\mathbf{r} + E\left[\frac{4}{3}\nabla(\nabla\cdot\mathbf{q}) - \nabla\times(\nabla\times\mathbf{q})\right] - |\varepsilon|\beta\nabla\cdot(\alpha(1-\alpha)\mathbf{q}_R\mathbf{q}_R)$$

where

$$E = \frac{\mu^*}{\rho_C^*\Omega^* r_0^{*2}}, \qquad P = \frac{1}{(\Omega^* r_0^*)^2|\varepsilon|}\frac{P^*}{\rho_C^*} - \frac{1}{2}\Omega^{*2}r^{*2}, \qquad s = \varepsilon/|\varepsilon|$$

and μ^* is the effective viscosity of the mixture.

Assume that the viscious forces are small compared to the Coriolis force (*2*) (i.e., the Ekman number, E, is small), the Coriolis force is small compared to the Stokes drag on a particle (i.e., β is small), and the momentum-diffusion term and inertial terms in the momentum equation are negligible. Then the momentum equation represents the balance of Coriolis force by an azimuthal pressure gradient and bouyancy by drag.

A section of a representative centrifuge with a meridional barrier is shown in Fig. 2, with dimensionless inner radius r_i and outer radius 1. The top and bottom are described by the equations $z = z_T(r)$ and $z = z_B(r)$, respectively, with angles of inclination $\gamma_T(r)$ and $\gamma_B(r)$. Greenspan and Ungarish used the reduced momentum equation and the continuity equations to show that, to a first-order approximation in β, if the initial volume fraction, α_I, is independent of z and θ, then α and j_r are also independent of z and θ. If α_I is uniform (i.e., the mixture is initially homogeneous), then α within the mixture region is a function only of time and j_r is independent of z. In what follows, we deal only with initially homogeneous mixtures.

Assume for definiteness that the dispersed phase is denser than the continuous phase. Then a core of pure fluid forms during separation. Let R denote the position of its interface with the mixture region and let S denote the thickness of the sediment on the outer wall. Then R and S are functions only of time. Also, define Q by $Q(r,t) = r < j_{r0} > (r,t)$, where j_{r0} is the approximation (to first order in β) to j_r and $<j_{r0}>$ is the azimuthally averaged value of j_{r0}.

Assuming the sediment layer on an inwardly inclined portion of a lid is

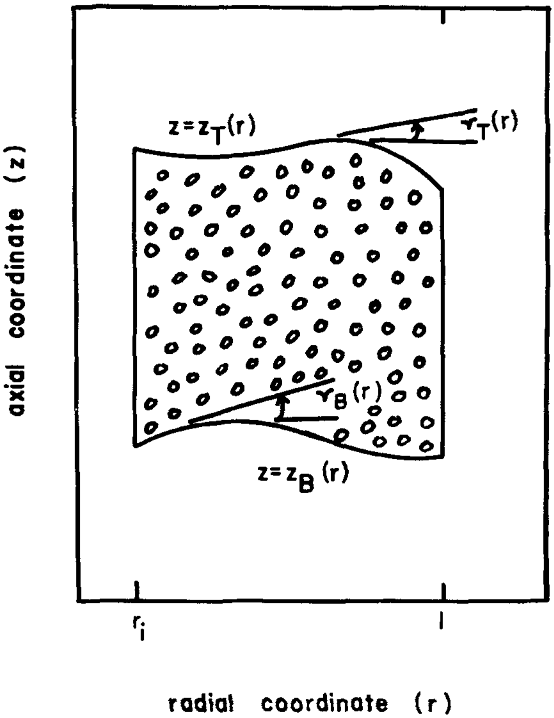

FIG. 2. Initial centrifuge configuration.

thin, the boundary condition there would be $\mathbf{j}\cdot\mathbf{n} = 0$ where $\mathbf{n}$ is a unit normal to the lid. A thin inviscid layer of pure fluid forms on outwardly inclined portions if $E^{1/2}/\beta \ll 1$ and $|\varepsilon| = 0(1)$. This is joined to the mixture by a thinner, inviscid layer with negligible mass flux. Thus the boundary condition there would be $\mathbf{j}_D\cdot\mathbf{n} = 0$.

Greenspan and Ungarish reduce the momentum equation and continuity equations to differential equations for α, Q, and R. For α_I constant and all quantities azimuthally averaged, their equations reduce to the following. The continuity equation (2.1) implies

$$\frac{d\alpha(t)}{dt} + 2\phi(\alpha(t)) = 0, \qquad \alpha(0) = \alpha_I \tag{2.3}$$

where $\phi(\alpha) = \alpha(1-\alpha)f(\alpha)$. The continuity equation (2.2) and the boundary conditions give

$$Q(r,t) + \left[z_k \frac{\partial Q(r,t)}{\partial r} + rC(r,t)\right] \cot \gamma_k(r) + \sigma_k(r) r^2 \frac{\phi(\alpha(t))}{\alpha(t)} = 0$$

$$Q(1 - S(t),t) = 0$$

for $k = T$ and B, where C is a constant of intergration which depends on the geometry of the centrifuge and where

$$\sigma_k = \begin{cases} 0 \text{ for inwardly inclined lids} \\ 1 \text{ for outwardly inclined lids} \end{cases} \quad \text{for } k = T \text{ and } B \quad .$$

Combining the equations for the top and bottom to eliminate C, we obtain

$$\frac{\partial Q}{\partial r} = \frac{-1}{z_T - z_B}\left\{Q[\tan \gamma_T - \tan \gamma_B] + r^2 \frac{\phi(\alpha)}{\alpha}[\sigma_T \tan \gamma_T - \sigma_B \tan \gamma_B]\right\}$$

$$Q(1 - S(t),t) = 0 \tag{2.4}$$

Since the velocity of the pure fluid-mixture interface is the velocity of the particles at the interface, one obtains the equation

$$\frac{dR(t)}{dt} = \frac{\phi(\alpha(t))}{\alpha(t)} R(t) + \frac{Q(R(t),t)}{R(t)}, \qquad R(0) = r_i \tag{2.5}$$

Equations (2.3), (2.4), and (2.5), along with the explicit formula for S,

$$S(t) = 1 - \sqrt{\frac{\alpha_M - \alpha_I}{\alpha_M - \alpha(t)}}$$

determine R. Then R can be used to calculate the fraction of the particles, F, which have settled:

$$F(t) = 1 - \frac{\alpha(t) \int_{R(t)}^{1-S(t)} [z_T(r) - z_B(r)] r dr}{\alpha_I \int_{r_I}^{1} [z_T(r) - z_B(r)] r dr} \tag{2.6}$$

We seek to compute, as a figure of merit for any given centrifuge configuration, the time t_s at which 95% of the particles have been separated.

3. APPROXIMATE SOLUTION PROCEDURE

To find t_s, we apply a root-finding method, such as Newton's method or the bisection method, to $F(t) - 0.95 = 0$. This requires that we be able to evaluate $R(t)$ for any t. To this end we first numerically solve (2.3) at specified grid points and construct an interpolate for α. To evaluate $R(t)$, we numerically integrate (2.5) up to t. The singularity can be eliminated by replacing the differential equation for R with a differential equation for R^2. If an explicit method is used to solve the equation approximately, at each time step the right-hand side of (2.5) is evaluated at previously calculated values of R. At each of these time steps an ordinary differential equation solver is used to solve (2.4) with time as a parameter, integrating from

$$1 - S(t) = \sqrt{(\alpha_M - \alpha_I)/(\alpha_M - \alpha(t))}$$

to the previously calculated value of R.

An error estimate is given, without proof, in the following theorem.

Theorem. Suppose the step sizes in the differential equation solvers for (2.3), (2.4), and (2.5) are all $O(h)$, the local errors are $O(h^{r+1})$, the global errors are $O(h^r)$, and the error in interpolating α is $O(h^r)$. Then for any t, the error in approximately calculating $F(t)$ using the above algorithm is $O(h^r)$.

The authors used a cubic spline to interpolate α (with error $O(h^4)$) and variable order step-size fifth- and sixth-order Runge-Kutta-Fehlberg methods to solve the differential equations numerically. Thus, the error in $F(t)$ was $O(h^4)$). The maximum step size was $h = 0.1$.

4. RESULTS

Several series of tests were run to show the effects of various aspects of the geometry of the centrifuge on the time required for 95% separation to occur. All quantities given are dimensionless unless otherwise stated. In all cases, α_M was chosen to be 1 (*3*). Table 1 shows the effect of α_I on the separation time for the centrifuge in Fig. 3 with $H = 1$. In all subsequent computations, α_I is chosen to be 0.0002.

The results in Table 2 show the effect of the inner radius on the separation time for centrifuges with horizontal lids (Fig. 4). With horizontal lids, the dependent variables, α, Q, R, and t_s, are independent

TABLE 1
Height of 1, Endcap Slope of 1, Zero Inner Radius, and Various Initial Concentrations (Fig. 3)

α_I	t_s
0.00002	0.6777
0.0002	0.6780
0.002	0.6814
0.02	0.7164

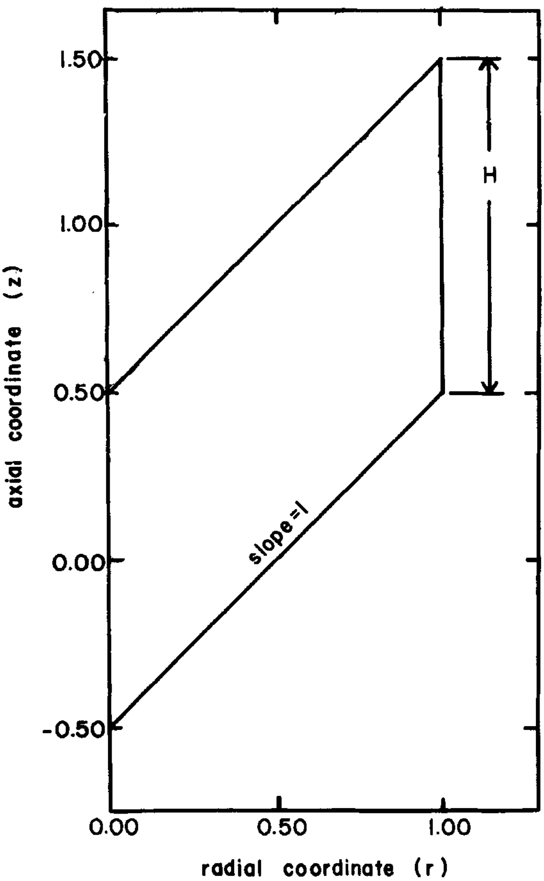

FIGURE. 3.

TABLE 2
Horizontal Endcaps with Various Inner Radii (Fig. 4)

r_I	t_s	$R(t_s)$
0.0	1.495964	0.0
0.0001	1.495965	0.000448
0.001	1.495959	0.004480
0.01	1.495251	0.044352
0.1	1.411147	0.409422
0.2	1.215510	0.670422
0.4	0.800125	0.889897

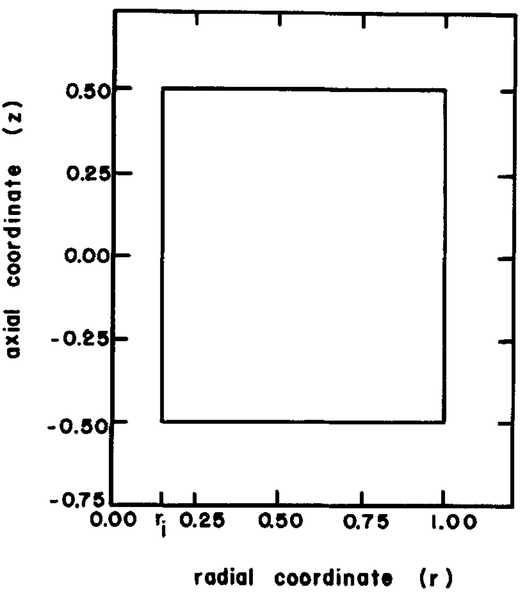

FIGURE. 4.

of the height of the centrifuge (cf. Eq. 2.4 with $\gamma_T = \gamma_B = 0$). When $r_i = 0$, no central core of pure fluid is formed (*4*), as was stated in Ref. *1*, where the separation time was determined analytically in the limit $\alpha_l \rightarrow 0$ for $r_i = 0$. For $r_i \neq 0$, an inner core of pure fluid forms, shortening the separation time. The value of α in the mixture region is unaffected since the solution of (2.3) does not depend on the geometry of the centrifuge. However, Q and R are affected by z_T, z_B, and r_i.

The next series (Fig. 3 and Table 3) reproduces results obtained in the limit $\alpha_l \rightarrow 0$ in Ref. *1*. Greenspan and Ungarish showed that the separation time depends on $H \cot \gamma$ so that the decrease in t_s could have been obtained by increasing the slope rather than decreasing the height.

The results in Table 4 for the geometry of Fig. 5 show that enhancement gained by choosing $r_i \neq 0$ is not significant compared to the enhancement due to the Boycott effect. Therefore, r_i is taken to be zero in the computer runs reported below.

The next several sets of experiments show the effect of curved lids on the Boycott effect. First, parallel parabolic curves are superimposed on a centrifuge with a slope of 1 and a height of 1, as in Fig. 6. The separation time was $t_s = 0.84$ as compared to $t_s = 0.68$ for the centrifuge with linear lids of slope 1. It appears that the curvature interferes with the Boycott effect. With the nonparallel parabolic lids superimposed on a slope of 1 in Fig. 7, the result is even worse, $t_s = 1.11$.

In order to determine the effect of the amount of perturbation from linear lids on the separation time, curves, each of which were one-half period of a sine curve, with various amplitudes were superimposed on a slope of 1. For parallel curves, as in Fig. 8, the separation time increases for small to moderate perturbations from linear lids (Table 5), presumably due to interference with the Boycott effect. For large amplitudes, the separation time improves. This may be due to the large increase in the surface area available for sedimentation or due to the increase in the effective slopes of the lids due to their curvature. Nonparallel sine curves were also superimposed on a slope of 1 (Fig. 9). The heights of the

TABLE 3
Various Heights and Endcap Slope of 1 (Fig. 3)

H	t_s
2.0	0.87
1.0	0.68
0.4	0.44
0.2	0.30

TABLE 4
Height of 1, Endcap Slope of 1, and Various Inner Radii (Fig. 5)

r_I	t_s
0.0	0.6780432
0.0001	0.6780421
0.001	0.6780407
0.01	0.6779274
0.1	0.6668140
0.2	0.6340866

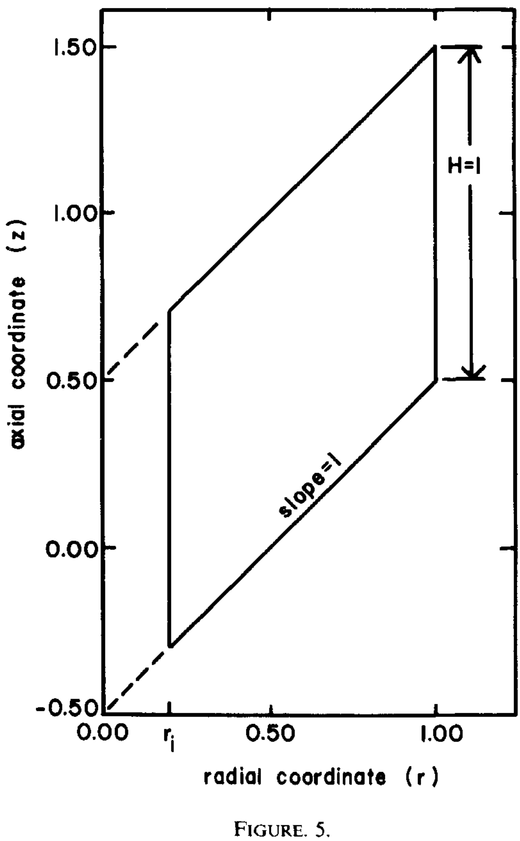

FIGURE. 5.

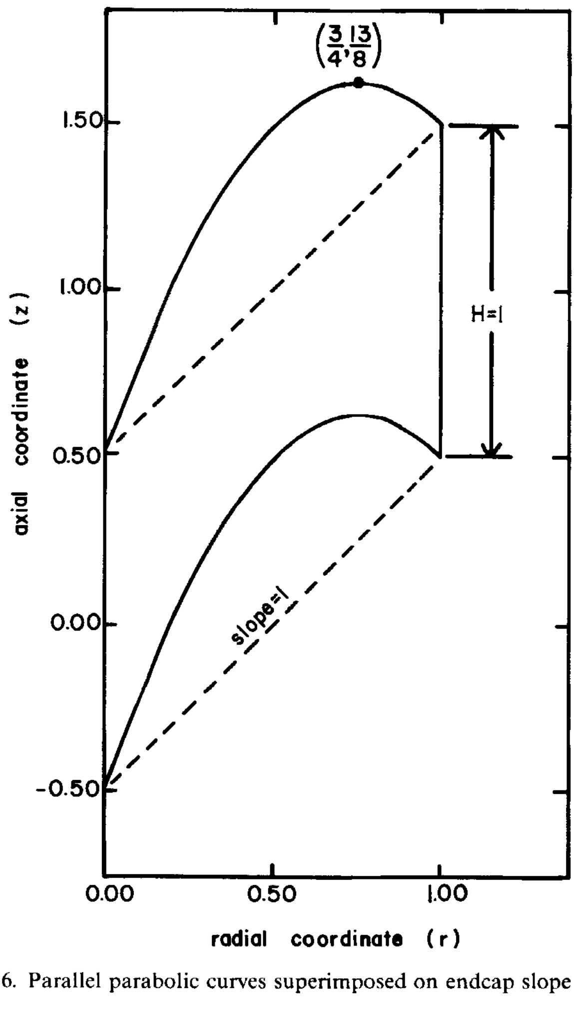

FIG. 6. Parallel parabolic curves superimposed on endcap slope of 1.

centrifuges were adjusted to maintain a constant volume for all amplitudes. The interference with the Boycott effect (see Table 6) is the same as it was for the parallel lids in Table 5.

The effect of introducing curvature to horizontal lids was also studied. Sine curves with various amplitudes were superimposed on horizontal lids (Fig. 10). The parallel lids show increasing improvement in the separation time as the amplitude increases (Table 7), presumably for the same reason that large perturbations from linear lids enhance separation (cf. Table 5). The nonparallel lids with constant volume (Fig. 11) also

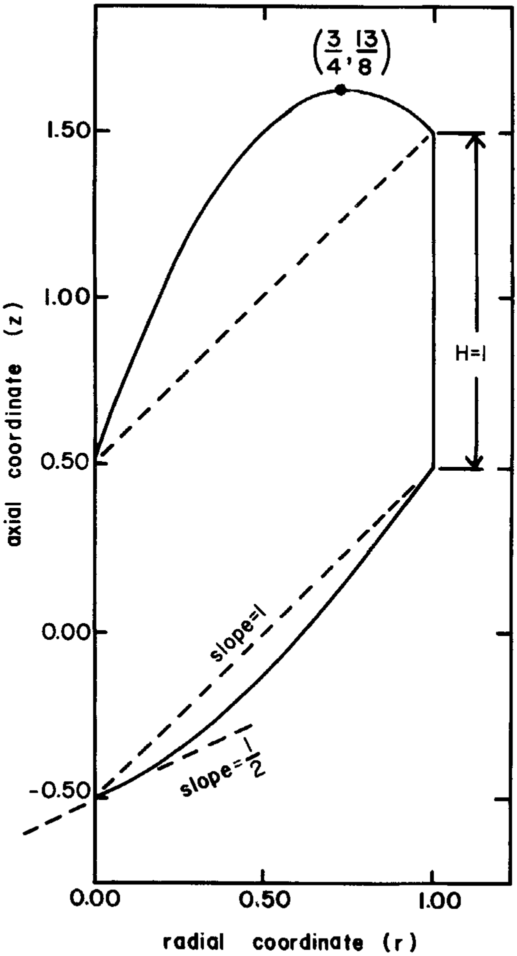

FIG. 7. Nonparallel parabolic curves superimposed on endcap slope of 1.

show improvement with increasing amplitude (Table 8), but the improvement is not as great as is that for the parallel lids.

The final set of numerical experiments utilized centrifuges in which a sawtooth pattern was superimposed on centrifuges with slope 1 and height 1. A series of tests was made with parallel lids and with the sawteeth having alternating slopes of 5 and −3. A cross section of a representative centrifuge, with four teeth, is shown in Fig. 12. Note that the height of the teeth decreases as the number of teeth increases. The

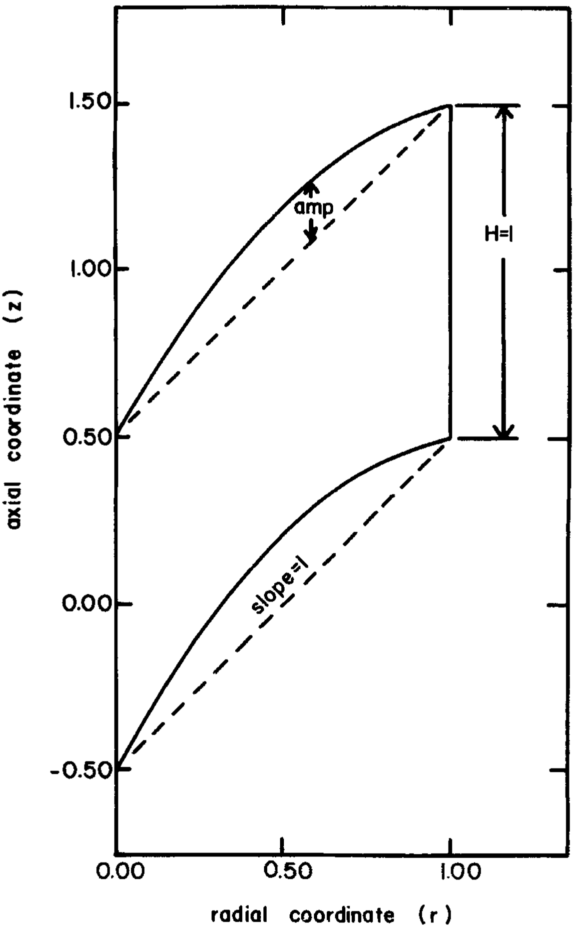

FIG. 8. Sine curves superimposed on endcap slope of 1.

TABLE 5
Parallel Sine Curves Superimposed on Endcap Slope of 1 (Fig. 8)

Amp	t_s
0.0	0.68
0.1	0.75
0.2	0.84
0.4	0.98
0.8	0.65
1.6	0.39

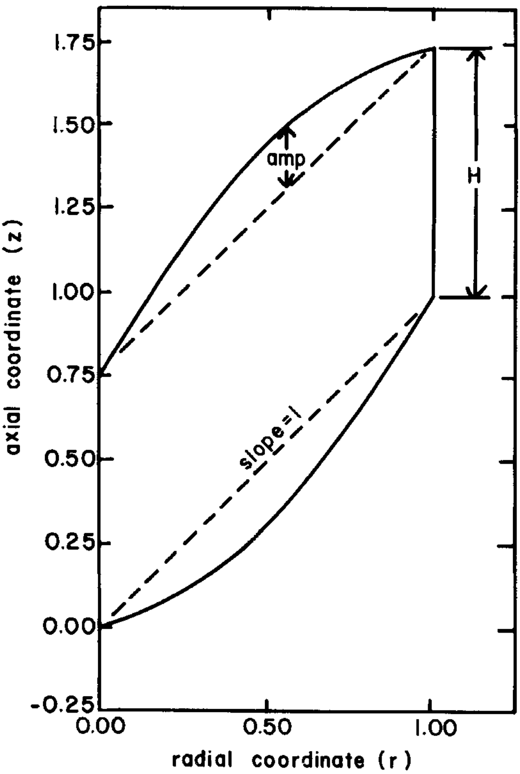

FIG. 9. Nonparallel sine curves superimposed on endcap slope of 1. $H = 1 - 4\ \text{amp}/\pi$.

TABLE 6
Nonparallel Sine Curves Superimposed on Endcap Slope of 1 (Fig. 9)

Amp	t_s
0.0	0.68
0.1	0.75
0.2	0.83
0.4	1.01

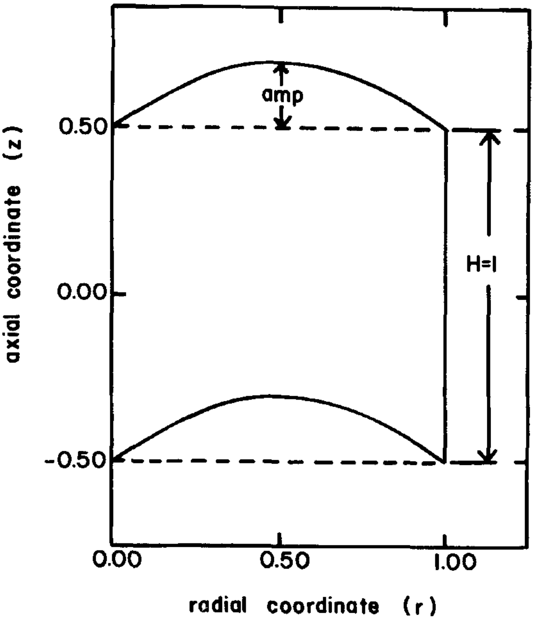

FIG. 10. Sine curves superimposed on horizontal endcaps.

TABLE 7
Parallel Sine Curves Superimposed on Endcap Slope of 0 (Fig. 10)

Amp	t_s
0.0	1.50
0.1	1.09
0.2	0.90
0.4	0.69
0.8	0.50
1.6	0.34

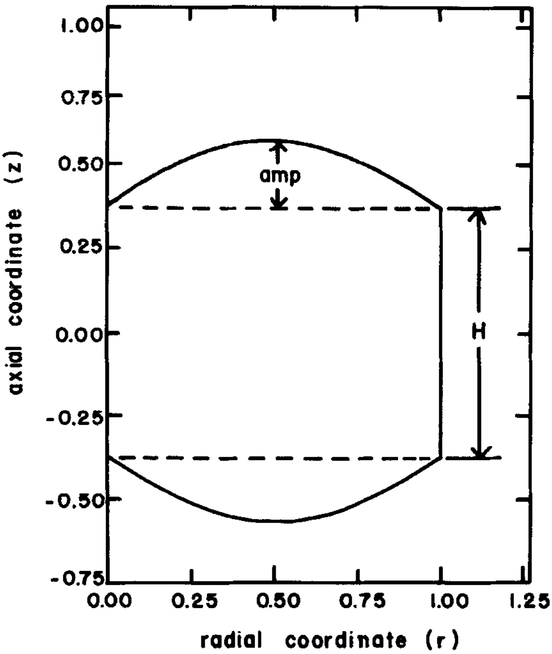

FIG. 11. Nonparallel sine curves superimposed on horizontal endcaps. $H = 1 - 4\ \text{amp}/\pi$.

TABLE 8
Nonparallel Sine Curves Superimposed on Endcap Slope at 0 (Fig. 11)

Amp	t_s
0.0	1.50
0.1	1.41
0.2	1.34
0.4	1.23

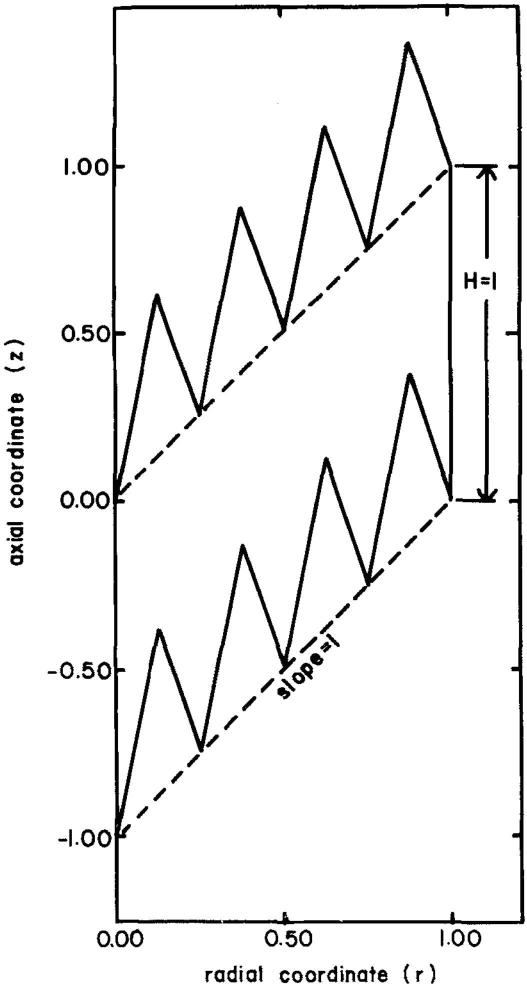

FIG. 12. Parallel sawteeth with alternating slopes of 5 and −3 superimposed on endcap slope of 1.

separation time improves as the number of teeth increases (see Table 9). For shallower teeth, with alternating slopes of 3 and −1, the improvement is not as great. With 10 teeth, the separation time was $t_s = 0.52$, which is worse than the time, $t_s = 0.35$, for the steeper teeth, but still better than the separation time for no teeth (cf. Table 9). The configuration in Fig. 13, having nonparallel teeth, was also tested. The separation time, $t_s = 0.98$, is worse than that with no teeth.

TABLE 9
Parallel Sawtooth Lids with Alternating Endcap Slopes of 5 and −3 (Fig. 12)

Number of teeth	t_s
0	0.68
1	0.40
2	0.37
10	0.35
20	0.34

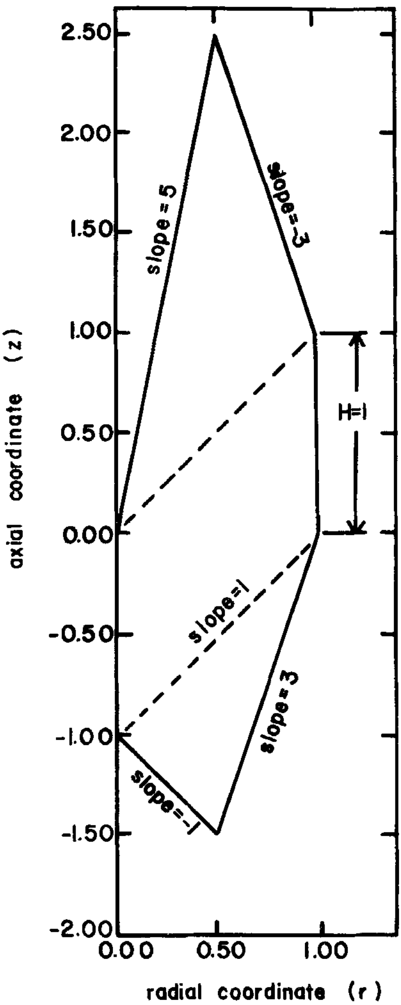

FIG. 13. Nonparallel sawteeth superimposed on endcap slope of 1.

5. CONCLUSIONS

The centrifuge shapes studied were not selected for ease of manufacture. However, our study illustrates some aspects of the shape dependence of separation. We confirm the results of Greenspan and Ungarish (*1*): nonhorizontal lids are superior to horizontal lids. Here we have demonstrated that a nonzero inner radius is less effective than sloped lids in enhancing the separation. Furthermore, although superimposing a moderate curve onto a slope interferes with the Boycott effect, a large curve or a sawtooth can improve the separation time. Finally, in all of the above studies, parallel lids performed as well as, indeed usually better than, nonparallel lids.

Acknowledgment

This work was supported by a grant from James Madison Univeristy Program of Grants for Faculty Research. The authors wish to thank Houston G. Wood and R. J. Ribando for their guidance and helpful suggestions, Henry W. Leap and R. Mark Freeman for their patient drawings of the figures, and the Academic Computer Center at James Madison University for their willing service. Numerical computations were performed on James Madison University's VAX 8600.

REFERENCES

1. H. P. Greenspan and M. Ungarish, *J. Fluid Mech., 157,* 359 (1985).
2. A. Acrivos and E. Herbolzheimer, *Ibid., 92,* 435 (1979).
3. H. P. Greenspan and M. Ungarish, *Int. J. Multiphase Flow, 11,* 825 (1985).
4. M. Ishii and T. C. Chawla, *Local Drag Laws in Dispersed Two-Phase Flow,* Argonne National Lab. ANL-79-105, 1979.
5. M. Ungarish, *Phys. Fluids, 29,* 640 (1986).
6. D. Hilbert and S. Cohn-Vossen, *Geometry and the Imagination,* Chelsea, New York, 1952.

Received by editor November 3, 1986